Schisandrin A protects against isoproterenol-induced chronic heart failure via miR-155

LIJING GAO, TING LI, SHUFEN LI, ZHUOHUI SONG, YONGLI CHANG and LI YUAN

Medical College, Changzhi Medical College, Changzhi, Shanxi 046000, P.R. China

Received April 26, 2021; Accepted September 27, 2021

DOI: 10.3892/mmr.2021.12540

Abstract. Schisandrin A (Sch A) has a protective effect on cardiomyocytes. Circulating miR-155 levels are related to chronic heart failure (CHF). The present study aimed to clarify the role and the molecular mechanism of Sch A in CHF. C57BL/6JGpt mice were used for an isoproterenol (ISO)-induced CHF model to collect heart samples. Echocardiography was employed to detect heartbeat indicators. The degree of myocardial hypertrophy was evaluated based on the measurement of heart weight (HW), body weight (BW) and tibia length (TL) and the observation using hematoxylin-eosin staining. Sprague-Dawley rats were purchased for the separation of neonatal rat ventricular myocytes (NRVMs), which were treated with ISO for 24 h. Transfection regulated the level of miR-155. The viability of NRVMs was detected via MTT assay. The mRNA and protein levels were measured via reverse transcription-quantitative PCR and western blotting and immunofluorescence was used to detect the content of α-smooth muscle actin (α-SMA). Treatment with ISO resulted in rising left ventricular posterior wall thickness, intra-ventricular septum diastole, left ventricular end diastolic diameter, left ventricular end systolic diameter, HW/BW, HW/TL and falling ejection fraction and fractional shortening, the trend of which could be reversed by Sch A. Sch A ameliorated myocardial hypertrophy in CHF mice. In addition, Sch A inhibited ISO-induced upregulated expressions of atrial natriuretic peptide, B-type natriuretic peptide, B-myosin heavy chain and miR-155 in myocardial tissue. Based on the results *in vitro*, Sch A had no significant effect on the viability of NRVMs when its concentration was <24 μmol/l. Sch A inhibited the levels of miR-155, α-SMA and the phosphorylation levels of AKT and cyclic AMP response-element binding protein (CREB) in ISO-induced NRVMs, which was reversed by the upregulation of miR-155. Schisandrin A mediated the AKT/CREB signaling pathway to prevent CHF by regulating the expression of miR-155, which may shed light on a possible therapeutic target for CHF.

Correspondence to: Dr Li Yuan, Medical College, Changzhi Medical College, 161 Jiefang East Street, Changzhi, Shanxi 046000, P.R. China
E-mail: yuanlil_lly@163.com

Key words: chronic heart failure, schisandrin A, microRNA-155, isoproterenol, myocardial hypertrophys

Introduction

Chronic heart failure (CHF) is a clinical syndrome and heart abnormality is usually observed at the structural and functional levels (1). Cardiac output, cardiac contractility, filling pressure, wall stress during systolic and diastolic function and heart rhythm are the basis of the pathophysiology of CHF (2). A variety of pathological conditions, such as myocardial infarction, cardiomyopathy, hemodynamic overload and development of inflammation, can lead to decompensation of CHF (3,4). Once the heart is unable to maintain the peripheral blood perfusion of the whole body, it may cause mortality in patients (4). Due to the complexity of CHF, standardized and evidence-based treatment is essential (5).

In recent years, due to its special etiology, diagnosis and treatment systems, Traditional Chinese Medicine has received extensive attention, especially in the research of the mechanism of small molecule active ingredients (6,7). *Magnoliaceae schisandraceae* has a high medicinal value (8). Shengmai Yin (SMY), also known as pulse-activated decoction, is made of *Fructus schisandrae*, *Radix ginseng* and *Radix ophiopogonis* and is commonly used in the treatment of acute myocardial infarction, cardiogenic shock and arrhythmia (9,10). It is reported that SMY can alleviate the progression of adriamycin-induced CHF by suppressing pathological changes (10). Schisandrin A (Sch A) is one of the main active ingredients of lignans in *Schisandrin* and is a recognized monomer with pharmacological activity (11,12). A previous study noted that Sch A serves roles in the inhibition of inflammation and elimination of free radicals (13). In addition, Sch A suppresses lipopolysaccharide-induced inflammation and oxidative stress in macrophages *in vitro* (14). Moreover, Sch A can regulate bone metabolism (15), prevent cerebral ischemia reperfusion injury (16), attenuate acute liver injury (17) and acts against cancer (18). The present study focused on investigating the role and mechanism of Sch A in CHF.

Research on the mechanism of microRNAs (miRNAs, miRs) remains a popular and rewarding area of research. A number of reports have shown that miRNAs are involved in regulating the expression of specific genes and cellular processes in the process of CHF. For example, miR-129-5p

targets high mobility group box 1 to ameliorate heart function in CHF rats (19), miR-30d regulates cardiac remodeling (20) and miR-133a reduces cardiac hypertrophy by inhibiting the expressions of serum response factor and cyclin D2 (21). Upregulated miR-155 can be observed in a myocardial ischemia-reperfusion induction model (22) and circulating miR-155 levels may be a potential marker for the risk of arrhythmia in patients with CHF (23). miR-155 is encoded and co-expressed by the gene B-cell integration cluster and a previous study has indicated that Sch A regulates the proliferation and invasion of breast cancer cells through miR-155 (24).

Isoproterenol (ISO) is widely used to induce CHF (25). As such, it was hypothesized that the miR-155 may act as a downstream regulator of Sch A and participate in the treatment of CHF. An ISO-induced model was constructed and Sch A linked with miR-155 to explore the specific molecular mechanism of Sch A in the course of CHF for the first time, to the best of the authors' knowledge.

Materials and methods

Animals. A total of 50 male C57BL/6JGpt mice (10 weeks, 22-25 g) were purchased from GemPharmatech Co., Ltd., (cat. no. N000013) as the experimental subjects. All mice were adaptively reared under the specific pathogen-free (SPF) conditions of the animal facility (temperature, 23±2˚C; relative humidity, 45~70%; 12-h light/dark cycles) for 1 week. Mice were given free access to sufficient food and water.

All animal experiments were approved by the Ethic Committee of Experimental Animals of Changzhi Medical College (approval nos. M20200109 and R20200115; Changzhi, China).

Animal modeling. The mice were randomly divided into five groups, with 10 mice for each group as follows: i) CHF group, mice were slowly injected with ISO hydrochloride (cat. no. I5627; Merck KGaA) at a dosage of 30 mg/kg/day by the 2ML2 type ALZET osmotic pressure pump (DURECT Corporation) for 2 weeks to establish the CHF model (26); ii) control group, mice were injected with 0.9% normal saline (cat. no. D123478; The resources platform of the National standard material) including 0.002% ascorbic acid (cat. no. A92902; Merck KGaA) for 2 weeks; iii) Sch A-H group, mice were subjected to the procedures of the control group, except they also received intraperitoneal injections of Sch A (40 mg/kg/day; cat. no. HY-N0691; MedChemExpress) for 10 days (including modelling) in advance until the completion of modeling; iv) CHF + Sch A-L or v) CHF + Sch A-H group, mice were subjected to the procedures of the CHF group, except they also received intraperitoneal injections of Sch A (20 mg/kg/day or 40 mg/kg/day) for 10 days (including modelling) in advance until the modeling was completed (12).

Heartbeat index detection. After the completion of modeling, the mice were anesthetized by isoflurane (0.41 ml/min, at 4 l/min fresh gas flow; cat. no. 1349003; Merck KGaA) and fixed on the laboratory bench. The heartbeat indicators of each group of mice were detected by an echocardiography imaging system (VisualSonics, Inc.). Heartbeat indicators, including left ventricular end systolic diameter (LVESD; mm), left ventricular end diastolic diameter (LVEDD; mm), left ventricular posterior wall thickness (LVPWD; mm), intra-ventricular septum diastole (IVSD; mm), ejection fraction (EF; %) and fractional shortening (FS; %), were recorded and analyzed.

Cardiac physiological index test. The mice were sacrificed by anesthesia (Pentobarbital solution; cat. no. P-010-1ML; 60 mg/kg; Merck KGaA). Death was confirmed by observing whether the heartbeat had completely stopped and pupils were dilated. Afterwards, their body weight (BW) and tibia length (TL) were measured. Fresh hearts were quickly excised in a sterile environment and the heart weight (HW) was measured. Parts of the heart tissues were fixed at 4˚C with 4% paraformaldehyde (PFA; cat. no. 158127; Merck KGaA) for 2 h, dehydrated with alcohol (cat. no. PHR1070; Merck KGaA) followed by xylene (cat. no. B83606; Merck KGaA) and embedded in paraffin, and the remaining parts were ready for the extraction of RNA.

Pathological analysis of cardiac tissue. The paraffin-embedded heart tissue samples were sectioned (6 μm), deparaffinized and rehydrated. A hematoxylin-eosin staining (HE) staining kit (cat. no. AR1180; Boster Biological Technology) was used for staining. According to the manufacturer's protocols, at room temperature, the specimens were covered with hematoxylin staining solution for 3 min, Scott blue liquid (cat. no. G1865; Beijing Solarbio Science & Technology Co., Ltd.) for 1 min and eosin staining solution for 40 sec, respectively. Finally, the pathological abnormalities were observed under an inverted microscope (IXplore Pro; Olympus Corporation).

Quantification of mRNA level. Reverse transcription-quantitative (RT-q)PCR was performed to detect mRNA levels of miR-155, atrial natriuretic peptide (ANP), B-type natriuretic peptide (BNP) and B-myosin heavy chain (B-MHC). Primer3 Plus (http://www.primer3plus.com/cgi-bin/dev/primer3plus.cgi) was used to design the primers. According to the manufacturer's protocol, mouse myocardial tissues or isolated rat ventricular myocytes (NRVMs, $1x10^6$) were treated with TRIzol® (cat. no. 15596026; Thermo Fisher Scientific, Inc.) to extract total RNA. According to the manufacturer's protocol, reverse transcription of RNA was then performed using a miRNA reverse transcription kit (cat. no. 4366597; Thermo Fisher Scientific, Inc.) and PrimeScript RT-PCR kit (cat. no. RR014A; Takara Bio, Inc.). The cDNA was used as a template and RT-qPCR was performed on QuantStudio 3D PCR system (Thermo Fisher Scientific, Inc.) with QuantStudio 3D AnalysisSuite (Thermo Fisher Scientific, Inc.). qPCR thermocycling conditions were as follows: Denaturation at 94˚C for 5 min, 37 cycles of 95˚C for 15 sec, 60˚C for 30 sec and 72˚C for 30 sec. All reactions were repeated three times. U6 and GAPDH were the internal controls. The relative expressions of miR-155, ANP, BNP and B-MHC were expressed as a function of cycle quantification (Cq) and analyzed by the $2^{-\Delta\Delta Cq}$ method (27). The primers are listed in Table I.

Isolation and culture of ventricular myocytes. Sprague-Dawley (SD) rat pups (~2-3 days, Kaixue Biotechnology Co., Ltd.) were purchased to isolate NRVMs. After the rats were sacri-

Table I. Reverse transcription-quantitative PCR primers.

A, Gene (mouse)

Gene	Forward primer (5'→3')	Reverse primer (5'→3')
miR-155	UUAAUGCUAAUUGUGAUAGGGGU	TGTGACCCGAAAGCTCTA
ANP	AGGCAGTCGATTCTGCTT	CGTGATAGATGAAGGCAGGAAG
BNP	TAGCCAGTCTCCAGAGCAATTC	TTGGTCCTTCAAGAGCTGTCTC
B-MHC	TTGGATGAGCGACTCAAAAA	GCTCCTTGAGCTTCTTCTGC
GAPDH	TGCACCACCTGCTTAGC	GGCATGGACTGTGGTCATGAG
U6	GCTTCGGCAGCACATATACTA	CGAATTTGCGTGTCATCCTTG

B, Gene (rat)

Gene	Forward primer (5'→3')	Reverse primer (5'→3')
miR-155	AATGCTAATTGTGATAGGGG	GAACATGTCTGCGTATCTC
ANP-rat	GAGCAAATCCCGTATACAGTGC	ATCTTCTACCGGCATCTTCTCC
BNP-rat	GCTGCTGGAGCTGATAAGAGAA	GTTCTTTTGTAGGGCCTTGGTC
B-MHC	GAGGAGAGGGCGGACATT	ACTCTTCATTCAGGCCCTTG
GAPDH	GCAAGAGAGAGGCCCTCAG	TGTGAGGGAGATGCTCAGTG
U6	GGAACGATACAGAGAAGATTAGC	GGAACGATACAGAGAAGATTAGC

For single-stranded RNA miR-155, its forward primer was based on the sequences of stem-loop and miR-155 using Primer3 Plus (http://www.primer3plus.com/cgi-bin/ dev/primer3plus.cgi) and its reverse primer was designed in Primer3 Plus based on the stem-loop sequence and the complementary sequence of miR-155 sequence. miR, microRNA; ANP, atrial natriuretic peptide; BNP, B-type natriuretic peptide; B-MHC, B-myosin heavy chain.

ficed by anesthesia (pentobarbital solution, 50 mg/kg), fresh hearts were quickly excised in a sterile environment, followed by being minced and then lysed with 0.25% trypsin (cat. no. 25200056; Thermo Fisher Scientific, Inc.) until the tissue almost dissolved. Then, the cell suspension was centrifuged by a centrifuge (cat. no. TDL5M; Spring Instrument. Co., Ltd.) at 4,840 x g at room temperature for 5 min and the pellet was collected. The NRVMs were resuspended in DMEM/F12 (cat. no. A4192001; Thermo Fisher Scientific, Inc.) supplemented with 10% fetal bovine serum (FBS; AlphaCell) and streptomycin (100 U/ml; cat. no. 85886; Merck KGaA) and incubated in a humid incubator at 37˚C with 5% CO_2 (Heracell 150i CO_2 Incubator; cat. no. 51032719; Thermo Fisher Scientific, Inc.) (28).

Cell viability assay. NRVMs ($4x10^4$ cells) in logarithmic growth phase were seeded in each well of a 96-well plate (cat. no. HY-E0076, MedChemExpress) with culture medium containing 10% FBS and different concentrations of Sch A (0, 1, 2, 4, 8, 12 and 24 μM) and incubated at 37˚C with 5% CO_2 for 30 min. A total of three sets of parallel experiments were performed in each group in total. Next, MTT solution (cat. no. HY-15924, MedChemExpress) was added to each well and incubated with the cells at 37˚C for 4 h, followed by the addition of SDS (cat. no. 2-270-9; Qiguang Technology Trade). The OD value at an absorbance of 570 nm was measured in a microplate reader (SpectraMax iD5; Molecular Devices, LLC).

Cell grouping. The NRVMs in the ISO group were incubated with ISO (10 μM) only for 24 h at 37˚C. For the Sch A-4 group, the NRVMs were pretreated with Sch A (4 μM) for 30 min and then incubated with ISO (10 μM) for 24 h at 37˚C. For the Sch A-12 group, the NRVMs were pretreated with Sch A (12 μM) for 30 min and then incubated with ISO (10 μM) for 24 h at 37˚C (29).

Cell transfection. The transfection of miR-155 mimic [M; Sangon Biotech (Shanghai) Co., Ltd.] or miR-155 inhibitor [I; Sangon Biotech (Shanghai) Co., Ltd.] regulated the expression of miR-155, with the establishment of their corresponding control groups (transfection with non-sense sequence) [M control (MC) and I control (IC)]. miR-155 M or I was mixed with X-tremeGENE 9 DNA Transfection Reagent (cat. no. 6365787001; Merck KGaA) to configure the transfection complex, which was incubated at 25˚C for 15 min and added into the cell suspension ($1x10^5$) dropwise and continued to incubate at 37˚C for 48 h. The sequences were as follows: M, 5'-UUCCAAUGCUAAUUGUGAUAGGGGU-3'; I, 5'-ACCCCTATCACAATTAGCATTAA-3'; MC, 5'-AAGAAACCATGCAAAGTAAGGTT-3'; and IC, 5'-CCTAGGCTCACGTGACGCG-3'.

Immunofluorescence. The NRVMs were fixed at room temperature with 4% PFA on the glass slide for 15 min and then immersed in 0.5% Triton X-100 (cat. no. T8200; Beijing Solarbio Science & Technology Co., Ltd.) to permeate at room

temperature for 20 min. Normal goat serum (cat. no. ab7481; Abcam) was added to block cells at room temperature for 30 min. Then the antibody against α-smooth muscle actin (α-SMA; cat. no. 19245, Cell Signaling Technology, Inc.; 1:500) was added and incubated at 4˚C overnight. On the second day, Goat Anti-Rabbit IgG H&L (HRP; cat. no. 4412; Cell Signaling Technology, Inc.; 1:2,000) was added and incubated at 37˚C for 1 h. The subsequent steps were performed in the dark. DAPI (cat. no. 4083; Cell Signaling Technology, Inc.) was used to incubate at room temperature for 5 min for nuclear counterstaining. The collected images were captured under a fluorescence microscope (Dmi8; Leica Microsystems GmbH) and the results were expressed as average cell surface area (μm^2).

Western blotting. The NRVMs ($1x10^5$ cells) were mixed with the RIPA Lysis buffer (cat. no. 89901; Thermo Fisher Scientific, Inc.) to lyse protein for 10 min, followed by a centrifugation (3,000 x g) at 4˚C for 5 min. A bicinchoninic acid (BCA) kit (cat. no. P0011; Beyotime Institute of Biotechnology) was used to measure protein concentration. Denatured protein was mixed with 1X protein loading buffer [cat. no. C508320-0001; Sangon Biotech (Shanghai) Co., Ltd.]. The protein samples (30 μg/lane) were separated on 15% sodium dodecyl sulfate polyacrylamide gel electrophoresis (Bio-Rad Laboratories, Inc.) and then transferred to nitrocellulose membranes (cat. no. 1620090; Bio-Rad Laboratories, Inc.). Membranes were then blocked with 5% skimmed milk at room temperature for 2 h. The membranes were incubated with the diluted solution of primary antibodies, including protein kinase B (AKT; cat. no. ab8805; Abcam; 1:500; 60 kDa), phosphorylated (p)-AKT (cat. no. ab38449; Abcam; 1:1,000; 56 kDa), Cyclic AMP response-element binding protein (CREB; cat. no. ab32515; Abcam; 1:1,000; 40 kDa), p-CREB (ab32096; cat. no. Abcam; 1:5,00; 37 kDa), GAPDH (cat. no. ab181602; Abcam; 1:10,000; 36 kDa) at 4˚C overnight. The next day, the secondary antibody Goat Anti-Rabbit IgG H&L (cat. no. ab205718; Abcam; 1:50,000) was added for further 2 h incubation at room temperature. GAPDH was used as an internal control. Chromogenic liquid (cat. no. 34577; Thermo Fisher Scientific, Inc.) was used for the visualization in the dark, followed by the detection in an imaging system (Chemi Doc Touch; Bio-Rad Laboratories, Inc.), and the results were semi-quantified using ImageJ software (v1.8.0; National Institutes of Health).

Statistical analysis. Statistical analysis was performed by SPSS 20.0 (IBM Corp.). All experiments were repeated at least three times and the data are presented as the mean ± standard deviation. One-way analysis of variance was used for the comparison between multiple groups followed by Tukey's post hoc test. $P<0.05$ was considered to indicate a statistically significant difference.

Results

Sch A can ameliorate the gravimetric parameters of ISO-induced CHF mice. Following ISO treatment, echocardiography was used to assess the cardiac function of mice. Compared with normal mice, the indexes (LVPWD, IVSD, LVEDD and LVESD) of ISO-induced CHF mice were larger, while EF and FS were reduced ($P<0.01$; Fig. 1A-F). Meanwhile, it was found that Sch A treatment had no significant effect on normal mice, but it could partially reverse these indicators in CHF mice ($P<0.05$; Fig. 1A-F). Moreover, Sch A partially reversed the CHF-induced increased ratios of HW/BW and HW/TL ($P<0.05$; Fig. 1G and H). Pathologically, it could be observed that Sch A treatment alleviated the myocardial hypertrophy caused by CHF (Fig. 1I) and significantly reduced these adverse changes, with improved results represented following the treatment of higher concentration, suggesting that the therapeutic effect of Sch A was concentration-dependent (Fig. 1A-I).

Sch A can inhibit the expression of myocardial hypertrophy markers and miR-155. In the CHF mouse model, the expression levels of ANP, BNP and B-MHC were all increased, while Sch A treatment partially reduced the expression levels of these genes ($P<0.01$; Fig. 2A). Notably, Sch A could inhibit the upregulation of miR-155 in the CHF group ($P<0.01$; Fig. 2B). Similarly, high concentration of Sch A led to more obvious effects ($P<0.001$; Fig. 2A and B).

Interaction between Sch A and miR-155 in vitro. To determine the interaction between Sch A and miR-155, NRVMs were isolated from SD rat pups for cell experiments. The results of MTT test suggested that under the treatment of different gradients, Sch A significantly inhibited the cell viability of NRVMs when the concentration reached 24 μM ($P<0.05$; Fig. 3A). Therefore, the concentrations of 4 and 12 μM were chosen for follow-up experiments. Upregulation of miR-155 was also observed in ISO-treated cells, the trend of which was reversed by Sch A ($P<0.001$; Fig. 3B). As the inhibitory effect of the SchA-12 group was stronger than that of the SchA-4 group, the cells were subsequently treated with 12 μM SchA.

miR-155 M and I were designed to further investigate the role of miR-155 in CHF and its corresponding mechanism. The transfection of miR-155 M notably upregulated the expression level of miR-155, while miR-155 I led to a downregulation ($P<0.001$; Fig. 4A). The transfection of I also effectively attenuated the ISO-induced increase of miR-155 expression, the effects of which were similar to those of Sch A ($P<0.001$; Fig. 4B). The expression of miR-155 was promoted in the ISO + Sch A + M group when compared with the ISO + Sch A + MC group ($P<0.001$; Fig. 4B). Furthermore, it was demonstrated in the results of immunofluorescence that Sch A attenuated the promotive effects of ISO on the level of α-SMA ($P<0.001$; Fig. 4C and D). Downregulation of miR-155 also could inhibit ISO-induced increase of α-SMA content in NRVMs, while miR-155 M attenuated the inhibitory effect of Sch A on the level of α-SMA ($P<0.001$; Fig. 4C and D), suggesting that Sch A might regulate myocardial hypertrophy by inhibiting miR-155.

As for ANP, BNP, B-MHC, p-AKT and p-CREB, the transfection of miR-155 I attenuated the promotion of ISO, the effect of which was similar to that of Sch A and upregulating miR-155 expression attenuated the therapeutic effect of Sch A ($P<0.001$; Fig. 5A-D), suggesting that higher-expressed miR-155 could promote both the expressions of ANP, BNP, B-MHC and the phosphorylation of

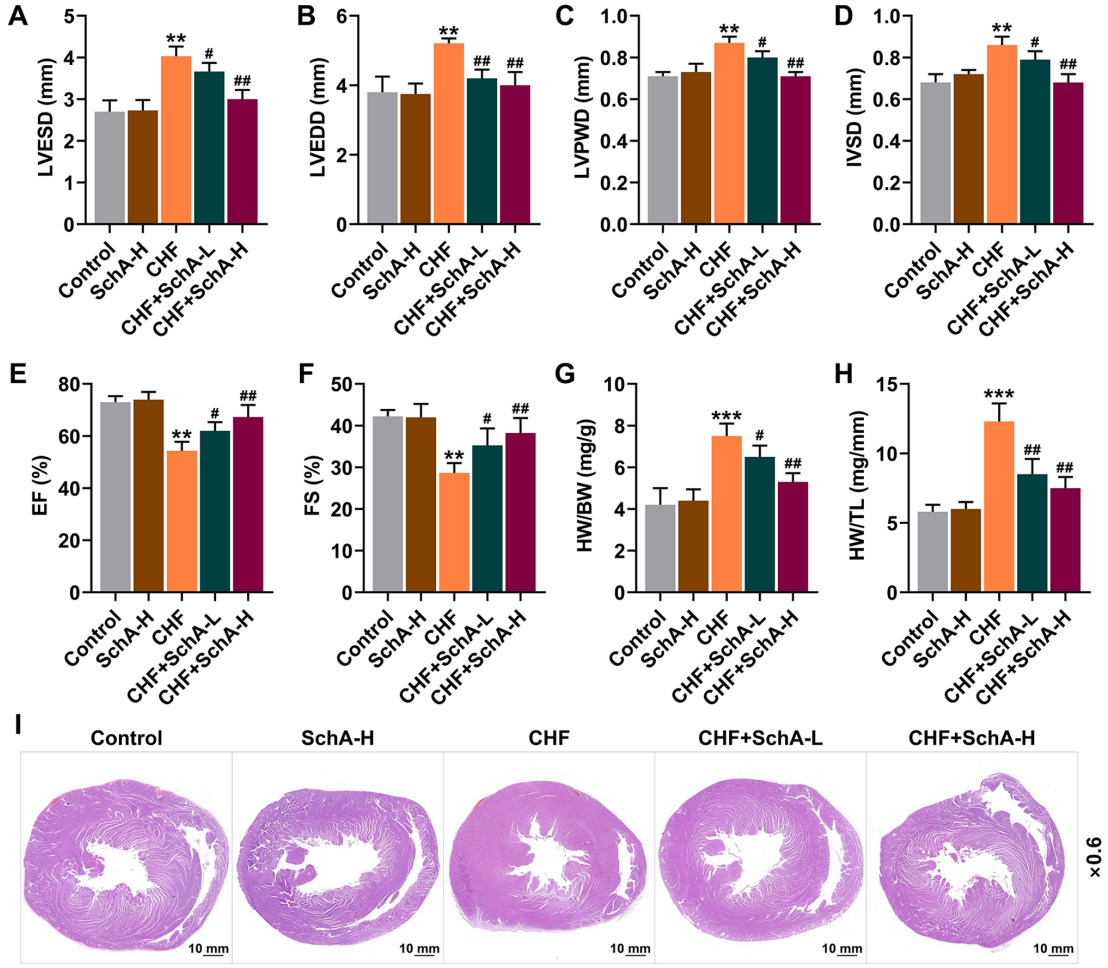

Figure 1. Sch A reverses the pathological changes induced by CHF. The levels of (A) LVESD, (B) LVEDD, (C) LVPWD, (D) IVSD, (E) EF and (F) FS were detected by echocardiography. (G) The ratio of HW to BW. (H) The ratio of HW to TL. (I) Pathological hematoxylin-eosin staining stained sections of heart tissue. Scale bar, 10 mm; magnification, x0.6. **P<0.01, ***P<0.001 vs. Control; $^{\#}$P<0.05, $^{\#\#}$P<0.01 vs. CHF. Sch A, Schisandrin A; CHF, chronic heart failure; LVESD, left ventricular end systolic diameter; LVEDD, left ventricular end diastolic diameter; LVPWD, left ventricular posterior wall thickness; IVSD, intra-ventricular septum diastole; EF, ejection fraction; FS, fractional shortening; HW, heart weight; BW, body weight; TL, tibia length; Sch A-H, injected intraperitoneally with 40 mg/kg/day Sch A; Sch A-L, injected intraperitoneally with 20 mg/kg/day Sch A.

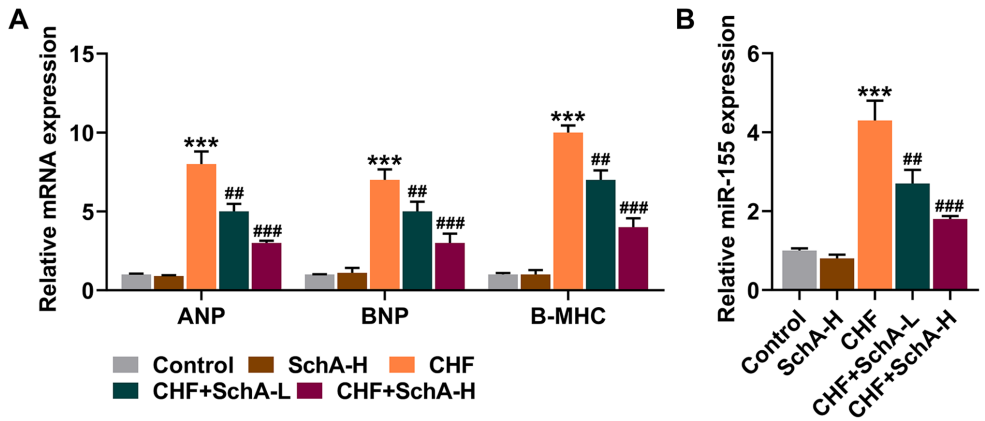

Figure 2. Sch A downregulates the expression levels of ANP, BNP, B-MHC and miR-155 induced by CHF. (A) mRNA expression levels of ANP, BNP and B-MHC in myocardial tissue were quantified by RT-qPCR. GAPDH was used as a control. (B) The expression of miR-155 in myocardial tissue was measured via RT-qPCR. U6 was used as a control. ***P<0.001 vs. Control; $^{\#\#}$P<0.01, $^{\#\#\#}$P<0.001 vs. CHF. Sch A, Schisandrin A; CHF, chronic heart failure; ANP, atrial natriuretic peptide; BNP, B-type natriuretic peptide; B-MHC, B-myosin heavy chain; miR, microRNA; RT-qPCR, reverse transcription-quantitative PCR; Sch A-H, injected intraperitoneally with 40 mg/kg/day Sch A; Sch A-L, injected intraperitoneally with 20 mg/kg/day Sch A.

AKT and CREB. The above evidence indicated that Sch A ameliorated ISO-induced hypertrophy in cardiomyocyte and inhibited the expressions of ANP, BNP, B-MHC, p-AKT and p-CREB via regulation of miR-155.

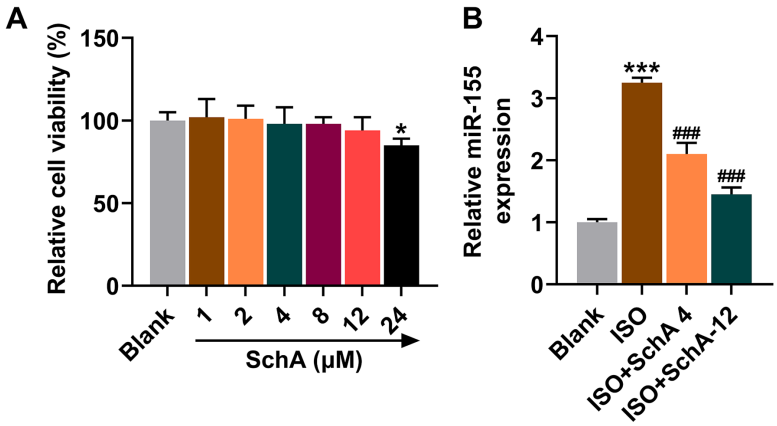

Figure 3. Effects of Sch A on rat NRVMs. (A) MTT was used to assess the effects of Sch A on the viability of cells. (B) The expression of miR-155 in rat NRVMs was calculated using reverse transcription-quantitative PCR with U6 as a control. *P<0.05, ***P<0.001 vs. Blank; $^{###}$P<0.001 vs. ISO. Sch A, Schisandrin A; NRVMs, neonatal rat ventricular myocytes; miR, microRNA; ISO, isoproterenol.

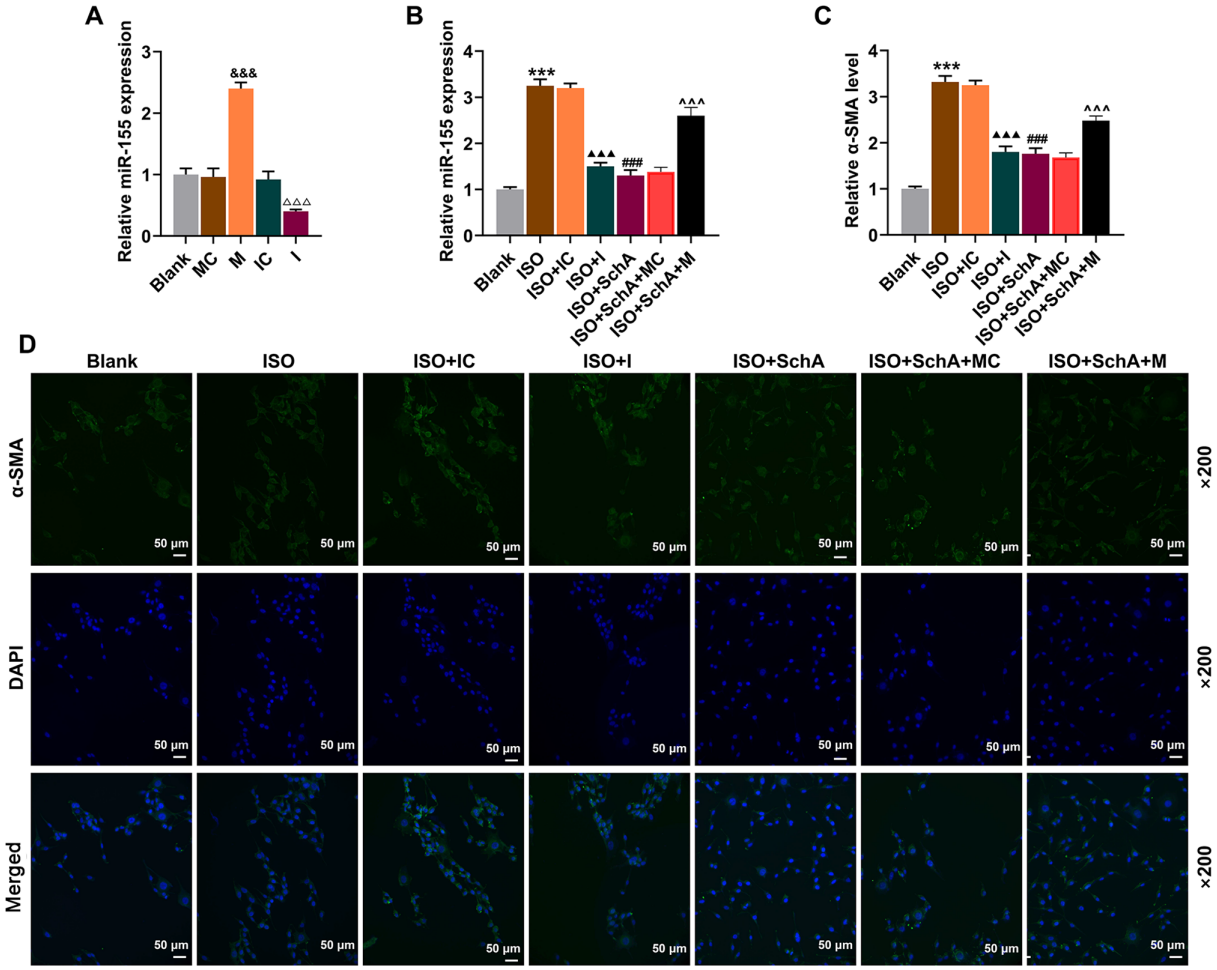

Figure 4. Sch A relieves fibrosis of neonatal rat ventricular myocytes via miR-155. (A) The transfection efficiency of miR-155 mimic or miR-155 inhibitor was evaluated by RT-qPCR. (B) The expression of miR-155 was determined via RT-qPCR. U6 was used as a control. (C and D) The level of α-SMA was observed by immunofluorescence. Scale bar, 50 μm; magnification, x200. $^{\&\&\&}$P<0.001 vs. MC; $^{\triangle\triangle\triangle}$P<0.001 vs. IC; ***P<0.001 vs. Blank; $^{\blacktriangle\blacktriangle\blacktriangle}$P<0.001 vs. ISO + IC; $^{###}$P<0.001 vs. ISO; $^{\wedge\wedge\wedge}$P<0.001 vs. ISO + Sch A + MC. Sch A, Schisandrin A; miR, microRNA; RT-qPCR, reverse transcription-quantitative PCR; α-SMA, α-smooth muscle actin; M, miR-155 mimic; MC, miR-155 mimic control; I, miR-155 inhibitor; IC, miR-155 inhibitor control; ISO, isoproterenol.

Discussion

Epidemiological data suggests that the prevalence of CHF is still rising, with high mortality and frequent hospitalizations (1). Echocardiography is the most useful and reliable non-invasive method for the diagnosis of cardiac insufficiency (3). Decreased myocardial contractility, abnormal hemodynamics and neuroendocrine activation are the distinctive features of CHF. In the

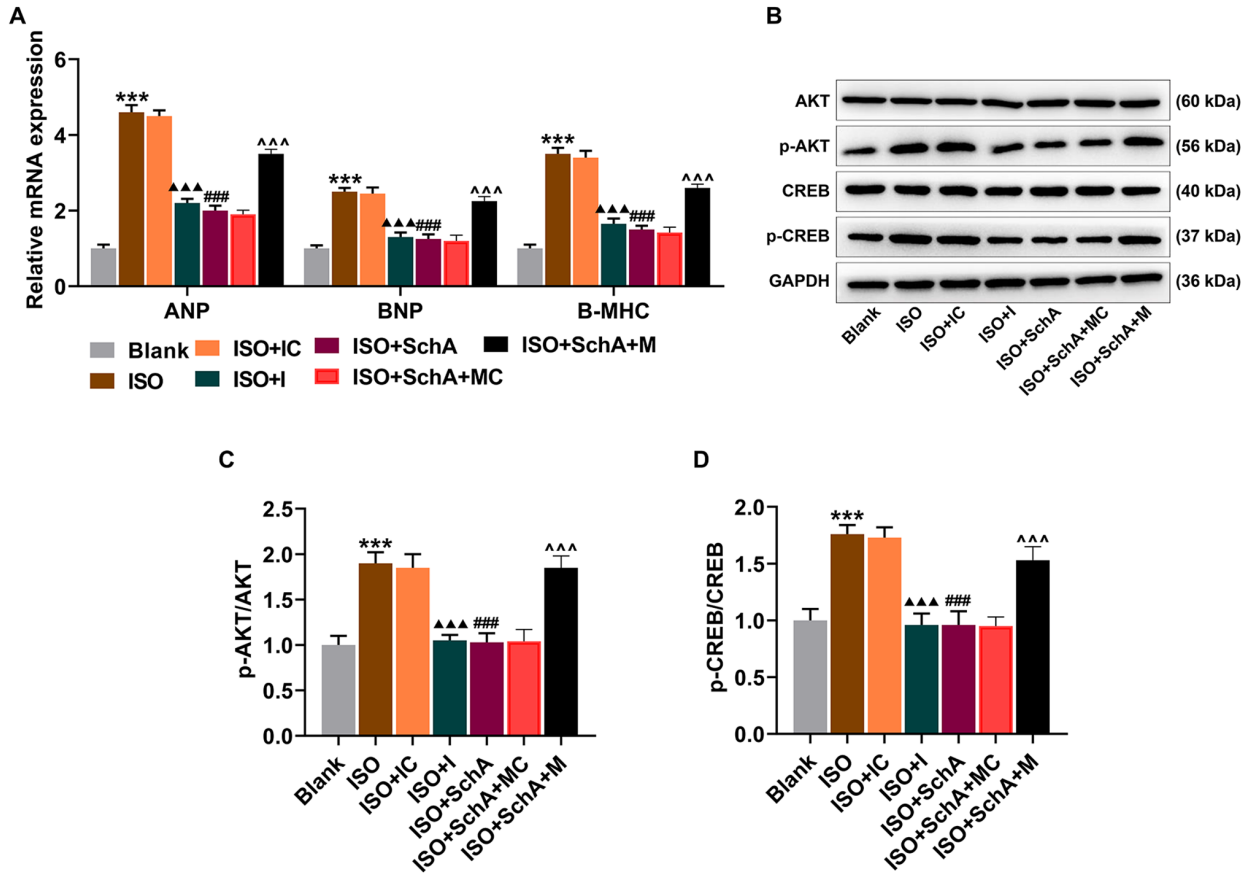

Figure 5. Sch A regulates ANP, BNP, B-MHC, pAKT/AKT and p-CREB/CREB via miR-155. (A) mRNA expression levels of ANP, BNP and B-MHC were measured using reverse transcription-quantitative PCR. GAPDH was used as a control. (B) The protein expression of AKT, p-AKT, CREB and p-CREB was semi-quantified by western blotting; GAPDH was used as a control. (C) The ratio of p-AKT to AKT. (D) The ratio of p-CREB to CREB. ***P<0.001 vs. Blank; ▲▲▲P<0.001 vs. ISO + IC; ###P<0.001 vs. ISO; ^^^P<0.001 vs. ISO + Sch A + MC. Sch A, Schisandrin A; miR, microRNA; ANP, atrial natriuretic peptide; BNP, B-type natriuretic peptide; B-MHC, B-myosin heavy chain; p-, phosphorylated; CREB, cyclic AMP response-element binding protein; M, miR-155 mimic; MC, miR-155 mimic control; I, miR-155 inhibitor; IC, miR-155 inhibitor control; ISO, isoproterenol.

current study, to obtain more evidence to further transform the application of Sch A in clinical patient management, mice were used to construct CHF models for *in vivo* and NRVMs isolated from rat pups for *in vitro*. Rat and mouse experiments are involved in the previous studies and, by contrast, the mouse CHF model is more mature, while the rat cell extraction is easier (30-32). The present study demonstrated the protective effects of Sch A in CHF via the administration of Sch A. The results of echocardiography showed that Sch A treatment alleviated ISO-induced heart damage, which was characterized by the reversal of LVPWD, IVSD, LVEDD, LVESD, EF and FS. In addition, it was found that Sch A ameliorated myocardial hypertrophy and reduced HW/BW, HW/TL in CHF mice. Myocardial hypertrophy, specifically referring to the increase in volume and weight of myocardial cells, rather than an increase in number (33), is an important compensation method for CHF in order to maintain the body's demand for cardiac output (33,34). The *in vivo* experiments of the present study supported the hypothesis that Sch A could prevent the ISO-induced deterioration in heart function and structure. CHF is the terminal stage of a number of diseases and neurohumoral activation is important for its diagnosis and prognosis (35). ANP and BNP belong to the family of natriuretic peptides and can be secreted by NRVMs (36,37). ANP can promote relaxation of vascular smooth muscles to stretch the heart wall and reduce blood pressure, which delays progress of CHF (38,39), while BNP has the effect of regulating the homeostasis of blood pressure and blood volume, which is used as a biochemical indicator as its concentration in plasma is directly proportional to the severity of CHF (40,41). In addition, B-MHC is specifically expressed in the heart of mammals and is closely related to cardiac function and myocardial hypertrophy (42,43). The present study observed that Sch A downregulated the mRNA levels of ANP, BNP and B-MHC in both CHF mouse model and cell model.

MicroRNA can be used as a biomarker and prognostic indicator of CHF in clinical applications (44). miR-155 is a conservative and multifunctional miRNA, which serves a non-negligible role in cancer (45), fibrotic diseases (46), lymphocyte homeostasis (47) and cardiovascular diseases (48). A study reports that the overexpression of miR-155 in human cardiomyocyte progenitor cells is associated with protection from necrotic cell death (49). Another report pointed out that inhibiting endogenous miR-155 may have a clinical potential to inhibit cardiac hypertrophy and CHF (50). The data from the present study demonstrated that Sch A specifically inhibited the ISO-induced upregulation of miR-155 *in vitro* and *in vivo*. α-SMA is known as a feature that distinguishes myofibroblasts (MF) from fibroblasts, which indicates the differentiation and maturity of MF (51). Based on the results

of immunofluorescence, it was shown that following SchA treatment, the intracellular level of α-SMA in ISO-treated NRVMs was downregulated, which was restored by inhibiting miR-155. The occurrence of fibrosis is one of the main factors of physiological cardiac hypertrophy and pathological cardiac hypertrophy (52,53). The present study revealed that Sch A could target miR-155 to alleviate pathological cardiac hypertrophy. In addition, it was found that miR-155 was not only associated with ANP, BNP and B-MHC, but was also involved in the activation of AKT and CREB signaling pathways. AKT is essential for the development of the heart and the insulin-like growth factor 1/PI3K/AKT pathway serves a key role in regulating exercise-induced physiological cardiac hypertrophy and cardioprotection (54). CREB is an important protein that regulates gene transcription, the transcription of which is regarded as a necessary regulator of the hypertrophic response (55,56). The present study demonstrated that blocking the activation of AKT/CREB counteracted the ISO-induced hypertrophy and Sch A inhibited the expression of miR-155, which thereby suppressed the phosphorylation of AKT and CREB.

Targeted therapy is a trend for precision medicine. In conclusion, the results of the present study provided evidence of the protective effect of Sch A on cardiac insufficiency and CHF remodeling, in addition to the revelation that Sch A-mediated downregulation of miR-155 was an essential mechanism implicated in the Sch A-mediated improvement of cardiac function, cardiac hypertrophy and fibrosis. Furthermore, *in vitro* experiments also demonstrated that Sch A inhibited the expression levels of ANP, BNP and B-MHC and blocked AKT/CREB activation via miR-155. This article provided a preliminary scientific basis for the clinical application of Sch A in CHF in the future.

Acknowledgements

Not applicable.

Funding

This work was supported by National Natural Science Foundation of China (grant no. 81902020), Scientific Research Project of Shanxi Provincial Health Commission (grant no. 2020135), Changzhi Medical College Doctor Startup Fund (grant no. BS17001) and Shanxi Province Applied Basic Research Project (grant no. 201901D211469).

Availability of data and materials

The datasets used and/or analyzed during the current study are available from the corresponding author on reasonable request.

Authors' contributions

LG made substantial contributions to conception and design. TL, SL, ZS, YC and LY performed data acquisition, analysis and interpretation. LG drafted the article and critically revised it for important intellectual content. LG and TL confirm the authenticity of all the raw data. All authors have read and approved the final manuscript.

Ethics approval and consent to participate

All animal experiments were approved by the Ethics Committee of Experimental Animals of Changzhi Medical College (approval nos. M20200109 and R20200115; Changzhi, China).

Patient consent for publication

Not applicable.

Competing interests

The authors declare that they have no competing interests.

References

1. Ewen S, Nikolovska A, Zivanovic I, Kindermann I and Böhm M: Chronic heart failure - new insights. Dtsch Med Wochenschr 141: 1560-1564, 2016 (In German).
2. Špinar J, Špinarová L and Vítovec J: Pathophysiology, causes and epidemiology of chronic heart failure. Vnitr Lek 64: 834-838, 2018.
3. King M, Kingery J and Casey B: Diagnosis and evaluation of heart failure. Am Fam Physician 85: 1161-1168, 2012.
4. Climent M, Viggiani G, Chen YW, Coulis G and Castaldi A: MicroRNA and ROS crosstalk in cardiac and pulmonary diseases. Int J Mol Sci 21: 21, 2020.
5. Dick SA and Epelman S: Chronic heart failure and inflammation: what do we really know? Circ Res 119: 159-176, 2016.
6. Wang J, Wong YK and Liao F: What has traditional Chinese medicine delivered for modern medicine? Expert Rev Mol Med 20: e4, 2018.
7. Zang Y, Wan J, Zhang Z, Huang S, Liu X and Zhang W: An updated role of astragaloside IV in heart failure. Biomed Pharmacother 126: 110012, 2020.
8. Rybnikář M, Šmejkal K and Žemlička M: Schisandra chinensis and its phytotherapeutical applications. Ceska Slov Farm 68: 95-118, 2019.
9. Ma S, Li X, Dong L, Zhu J, Zhang H and Jia Y: Protective effect of Sheng-Mai Yin, a traditional Chinese preparation, against doxorubicin-induced cardiac toxicity in rats. BMC Complement Altern Med 16: 61, 2016.
10. Zhang K, Zhang J, Wang X, Wang L, Pugliese M, Passantino A and Li J: Cardioprotection of Sheng Mai Yin a classic formula on adriamycin induced myocardial injury in Wistar rats. Phytomedicine 38: 1-11, 2018.
11. Xu D, Liu J, Ma H, Guo W, Wang J, Kan X, Li Y, Gong Q, Cao Y, Cheng J, *et al*: Schisandrin A protects against lipopolysaccharide-induced mastitis through activating Nrf2 signaling pathway and inducing autophagy. Int Immunopharmacol 78: 105983, 2020.
12. Zhi Y, Jin Y, Pan L, Zhang A and Liu F: Schisandrin A ameliorates MPTP-induced Parkinson's disease in a mouse model via regulation of brain autophagy. Arch Pharm Res 42: 1012-1020, 2019.
13. Cui L, Zhu W, Yang Z, Song X, Xu C, Cui Z and Xiang L: Evidence of anti-inflammatory activity of Schizandrin A in animal models of acute inflammation. Naunyn Schmiedebergs Arch Pharmacol 393: 2221-2229, 2020.
14. Kwon DH, Cha HJ, Choi EO, Leem SH, Kim GY, Moon SK, Chang YC, Yun SJ, Hwang HJ, Kim BW, *et al*: Schisandrin A suppresses lipopolysaccharide-induced inflammation and oxidative stress in RAW 264.7 macrophages by suppressing the NF-κB, MAPKs and PI3K/Akt pathways and activating Nrf2/HO-1 signaling. Int J Mol Med 41: 264-274, 2018.
15. Ni S, Qian Z, Yuan Y, Li D, Zhong Z, Ghorbani F, Zhang X, Zhang F, Zhang Z, Liu Z, *et al*: Schisandrin A restrains osteoclastogenesis by inhibiting reactive oxygen species and activating Nrf2 signalling. Cell Prolif 53: e12882, 2020.
16. Zhou F, Wang M, Ju J, Wang Y, Liu Z, Zhao X, Yan Y, Yan S, Luo X and Fang Y: Schizandrin A protects against cerebral ischemia-reperfusion injury by suppressing inflammation and oxidative stress and regulating the AMPK/Nrf2 pathway regulation. Am J Transl Res 11: 199-209, 2019.

17. Lu Y, Wang WJ, Song YZ and Liang ZQ: The protective mechanism of schisandrin A in d-galactosamine-induced acute liver injury through activation of autophagy. Pharm Biol 52: 1302-1307, 2014.
18. Xu X, Rajamanicham V, Xu S, Liu Z, Yan T, Liang G, Guo G, Zhou H and Wang Y: Schisandrin A inhibits triple negative breast cancer cells by regulating Wnt/ER stress signaling pathway. Biomed Pharmacother 115: 108922, 2019.
19. Xiao N, Zhang J, Chen C, Wan Y, Wang N and Yang J: miR-129-5p improves cardiac function in rats with chronic heart failure through targeting HMGB1. Mamm Genome 30: 276-288, 2019.
20. Li J, Salvador AM, Li G, Valkov N, Ziegler O, Yeri A, Yang Xiao C, Meechoovet B, Alsop E, Rodosthenous RS, *et al*: Mir-30d regulates cardiac remodeling by intracellular and paracrine signaling. Circ Res 128: e1-e23, 2021.
21. Wehbe N, Nasser SA, Pintus G, Badran A, Eid AH and Baydoun E: Micrornas in cardiac hypertrophy. Int J Mol Sci 20: 4714, 2019.
22. Ge X, Meng Q, Wei L, Liu J, Li M, Liang X, Lin F, Zhang Y, Li Y, Liu Z, *et al*: Myocardial ischemia-reperfusion induced cardiac extracellular vesicles harbour proinflammatory features and aggravate heart injury. J Extracell Vesicles 10: e12072, 2021.
23. Blanco RR, Austin H, Vest RN III, Valadri R, Li W, Lassegue B, Song Q, London B, Dudley SC, Bloom HL, *et al*: Angiotensin receptor type 1 single nucleotide polymorphism 1166A/C is associated with malignant arrhythmias and altered circulating miR-155 levels in patients with chronic heart failure. J Card Fail 18: 717-723, 2012.
24. Yan H and Guo M: Schizandrin A inhibits cellular phenotypes of breast cancer cells by repressing miR-155. IUBMB Life 72: 1640-1648, 2020.
25. Chang SC, Ren S, Rau CD and Wang JJ: Isoproterenol-induced heart failure mouse model using osmotic pump implantation. Methods Mol Biol 1816: 207-220, 2018.
26. Zhou Q, Pan LL, Xue R, Ni G, Duan Y, Bai Y, Shi C, Ren Z, Wu C, Li G, *et al*: The anti-microbial peptide LL-37/CRAMP levels are associated with acute heart failure and can attenuate cardiac dysfunction in multiple preclinical models of heart failure. Theranostics 10: 6167-6181, 2020.
27. Livak KJ and Schmittgen TD: Analysis of relative gene expression data using real-time quantitative PCR and the 2(-Delta Delta C(T)) method. Methods 25: 402-408, 2001.
28. Tan X, Li J, Wang X, Chen N, Cai B, Wang G, Shan H, Dong D, Liu Y, Li X, *et al*: Tanshinone IIA protects against cardiac hypertrophy via inhibiting calcineurin/NFATc3 pathway. Int J Biol Sci 7: 383-389, 2011.
29. Yang Y, Xu C, Tang S and Xia Z: Interleukin-9 Aggravates isoproterenol-induced heart failure by activating signal transducer and activator of transcription 3 signalling. Can J Cardiol 36: 1770-1781, 2020.
30. You X, Guo ZF, Cheng F, Yi B, Yang F, Liu X, Zhu N, Zhao X, Yan G, Ma XL, *et al*: Transcriptional up-regulation of relaxin-3 by Nur77 attenuates β-adrenergic agonist-induced apoptosis in cardiomyocytes. J Biol Chem 293: 14001-14011, 2018.
31. Cheng H, Wu X, Ni G, Wang S, Peng W, Zhang H, Gao J and Li X: *Citri Reticulatae* Pericarpium protects against isoproterenol-induced chronic heart failure via activation of PPARγ. Ann Transl Med 8: 1396, 2020.
32. Laudette M, Coluccia A, Sainte-Marie Y, Solari A, Fazal L, Sicard P, Silvestri R, Mialet-Perez J, Pons S, Ghaleb B, *et al*: Identification of a pharmacological inhibitor of Epac1 that protects the heart against acute and chronic models of cardiac stress. Cardiovasc Res 115: 1766-1777, 2019.
33. Gallo S, Vitacolonna A, Bonzano A, Comoglio P and Crepaldi T: ERK: A key player in the pathophysiology of cardiac hypertrophy. Int J Mol Sci 20: 20, 2019.
34. Heinzel FR, Hohendanner F, Jin G, Sedej S and Edelmann F: Myocardial hypertrophy and its role in heart failure with preserved ejection fraction. J Appl Physiol (1985) 119: 1233-1242, 2015.
35. Hartupee J and Mann DL: Neurohormonal activation in heart failure with reduced ejection fraction. Nat Rev Cardiol 14: 30-38, 2017.
36. Raveendran VV, Al-Haffar K, Kunhi M, Belhaj K, Al-Habeeb W, Al-Buraiki J, Eyjolsson A and Poizat C: Protein arginine methyltransferase 6 mediates cardiac hypertrophy by differential regulation of histone H3 arginine methylation. Heliyon 6: e03864, 2020.
37. Qi Y, Li JJ, Di XH, Zhang Y, Chen JL, Wu ZX, Man ZY, Bai RY, Lu F, Tong J, *et al*: Excess sarcoplasmic reticulum-mitochondria calcium transport induced by Sphingosine-1-phosphate contributes to cardiomyocyte hypertrophy. Biochim Biophys Acta Mol Cell Res 1868: 118970, 2021.
38. de Bold AJ: Atrial natriuretic factor: A hormone produced by the heart. Science 230: 767-770, 1985.
39. Charloux A, Piquard F, Doutreleau S, Brandenberger G and Geny B: Mechanisms of renal hyporesponsiveness to ANP in heart failure. Eur J Clin Invest 33: 769-778, 2003.
40. Gardner DG, Chen S, Glenn DJ and Grigsby CL: Molecular biology of the natriuretic peptide system: Implications for physiology and hypertension. Hypertension 49: 419-426, 2007.
41. Kuwahara K, Nakagawa Y and Nishikimi T: Cutting Edge of Brain Natriuretic Peptide (BNP) Research - The Diversity of BNP Immunoreactivity and Its Clinical Relevance. Circ J 82: 2455-2461, 2018.
42. Ingles J, Doolan A, Chiu C, Seidman J, Seidman C and Semsarian C: Compound and double mutations in patients with hypertrophic cardiomyopathy: Implications for genetic testing and counselling. J Med Genet 42: e59, 2005.
43. Hang CT, Yang J, Han P, Cheng HL, Shang C, Ashley E, Zhou B and Chang CP: Chromatin regulation by Brg1 underlies heart muscle development and disease. Nature 466: 62-67, 2010. Erratum in: Nature 475: 532, 2011.
44. Vegter EL, van der Meer P, de Windt LJ, Pinto YM and Voors AA: MicroRNAs in heart failure: From biomarker to target for therapy. Eur J Heart Fail 18: 457-468, 2016.
45. Michaille JJ, Awad H, Fortman EC, Efanov AA and Tili E: miR-155 expression in antitumor immunity: The higher the better? Genes Chromosomes Cancer 58: 208-218, 2019.
46. Eissa MG and Artlett CM: The microRNA miR-155 is essential in fibrosis. Noncoding RNA 5: 5, 2019.
47. Chen L, Gao D, Shao Z, Zheng Q and Yu Q: miR-155 indicates the fate of CD4+ T cells. Immunol Lett 224: 40-49, 2020.
48. Ding H, Wang Y, Hu L, Xue S, Wang Y, Zhang L, Zhang Y, Qi H, Yu H, Aung LHH, *et al*: Combined detection of miR-21-5p, miR-30a-3p, miR-30a-5p, miR-155-5p, miR-216a and miR-217 for screening of early heart failure diseases. Biosci Rep 40: BSR20191653, 2020.
49. Liu J, van Mil A, Vrijsen K, Zhao J, Gao L, Metz CH, Goumans MJ, Doevendans PA and Sluijter JP: MicroRNA-155 prevents necrotic cell death in human cardiomyocyte progenitor cells via targeting RIP1. J Cell Mol Med 15: 1474-1482, 2011.
50. Seok HY, Chen J, Kataoka M, Huang ZP, Ding J, Yan J, Hu X and Wang DZ: Loss of MicroRNA-155 protects the heart from pathological cardiac hypertrophy. Circ Res 114: 1585-1595, 2014.
51. Gabbiani G: The myofibroblast in wound healing and fibrocontractive diseases. J Pathol 200: 500-503, 2003.
52. Rai V, Sharma P, Agrawal S and Agrawal DK: Relevance of mouse models of cardiac fibrosis and hypertrophy in cardiac research. Mol Cell Biochem 424: 123-145, 2017.
53. McLellan MA, Skelly DA, Dona MSI, Squiers GT, Farrugia GE, Gaynor TL, Cohen CD, Pandey R, Diep H, Vinh A, *et al*: High-Resolution Transcriptomic Profiling of the Heart During Chronic Stress Reveals Cellular Drivers of Cardiac Fibrosis and Hypertrophy. Circulation 142: 1448-1463, 2020.
54. Weeks KL, Bernardo BC, Ooi JYY, Patterson NL and McMullen JR: The IGF1-PI3K-Akt Signaling Pathway in Mediating Exercise-Induced Cardiac Hypertrophy and Protection. Adv Exp Med Biol 1000: 187-210, 2017.
55. Jiang DS, Bian ZY, Zhang Y, Zhang SM, Liu Y, Zhang R, Chen Y, Yang Q, Zhang XD, Fan GC, *et al*: Role of interferon regulatory factor 4 in the regulation of pathological cardiac hypertrophy. Hypertension 61: 1193-1202, 2013.
56. Müller FU, Lewin G, Baba HA, Bokník P, Fabritz L, Kirchhefer U, Kirchhof P, Loser K, Matus M, Neumann J, *et al*: Heart-directed expression of a human cardiac isoform of cAMP-response element modulator in transgenic mice. J Biol Chem 280: 6906-6914, 2005.